Philosophical Magazine
Vol. 88, Nos. 13–15, 1–21 May 2008, 2261–2273

Taylor & Francis
Taylor & Francis Group

Electronic energy spectra of square and cubic Fibonacci quasicrystals

S. Even-Dar Mandel and R. Lifshitz*

Raymond and Beverly Sackler School of Physics and Astronomy Tel Aviv University, Tel Aviv 69978, Israel

(*Received 16 December 2007; final version received 16 March 2008*)

Understanding the electronic properties of quasicrystals, in particular the dependence of these properties on dimension, is among the interesting open problems in the field of quasicrystals. We investigate an off-diagonal tight-binding hamiltonian on the separable square and cubic Fibonacci quasicrystals. We use the well-studied Cantor-like energy spectrum of the one-dimensional Fibonacci quasicrystal to obtain exact results regarding the transitions between different spectral behaviours of the square and cubic quasicrystals. We use analytical results for the addition of one-dimensional spectra to obtain bounds on the range in which the higher-dimensional spectra contain an interval as a component. We also perform a direct numerical study of the spectra, obtaining good results for the square Fibonacci quasicrystal, and rough estimates for the cubic Fibonacci quasicrystal.

Keywords: Fibonacci quasicrystals; electronic spectra; electronic transport; quasicrystals

1. Background and motivation

As we celebrate the Silver Jubilee of the 1982 discovery of quasicrystals [1], and highlight the achievements of the past two and a half decades of research on quasicrystals, we are reminded that there still remains a disturbing gap in our understanding of their electronic properties. Among the open questions is a lack of understanding of the dependence of electronic properties – such as the nature of electronic wavefunctions, their energy spectra, and the nature of electronic transport – on the dimension of the quasicrystal. In an attempt to bridge some of this gap, we [2,3] have been studying the spectrum and electronic wavefunctions of an off-diagonal tight-binding hamiltonian on the separable n-dimensional Fibonacci quasicrystals[1] [4]. The advantage of using such separable models, despite the fact that they do not occur in nature, is the ability to obtain exact results in one, two, and three dimensions, and compare them directly to each other. Here we focus on the energy spectra of the two-dimensional (2D) and three-dimensional (3D) Fibonacci quasicrystals to obtain a quantitative understanding of the nature of the transitions between different spectral behaviours in these crystals, as their dimension increases from 1 up to 3. In particular, we consider the transitions between different regimes in the spectrum, taking into account the existence of a regime in which the

*Corresponding author. Email: ronlif@tau.ac.il

ISSN 1478–6435 print/ISSN 1478–6443 online

DOI: 10.1080/14786430802070805
http://www.informaworld.com

spectrum contains both continuous intervals and nowhere dense parts as components. These different behaviours of the higher-dimensional spectra are expected to reflect on the physical extent of the electronic wavefunctions, as well as on the dynamics of electronic wave packets, and are therefore of great importance in unravelling the electronic properties of quasicrystals in general.

Recall [2] that the off-diagonal tight-binding model assumes equal on-site energies (taken to be zero), and hopping that is restricted along tile edges, with amplitude 1 for long (L) edges and T for short (S) edges, where we take $T \geq 1$. The Schrödinger equation for the square Fibonacci quasicrystal in 2D (with obvious extensions to higher dimensions) is then given by

$$T_{n+1}\Psi(n+1,m) + T_n\Psi(n-1,m) + T_{m+1}\Psi(n,m+1) + T_m\Psi(n,m-1) = E\Psi(n,m), \quad (1)$$

where $\Psi(n,m)$ is the value of a 2D eigenfunction on a vertex labelled by the two integers n and m, and E is the corresponding eigenvalue. The hopping amplitudes T_j are equal to 1 or T according to the Fibonacci sequence $\{T_j\} = \{1, T, 1, 1, T, 1, T, 1, 1, T, 1, 1, T, 1, T, 1, 1, T, 1, T, \ldots\}$. By prohibiting diagonal hopping, the resulting high-dimensional eigenvalue problem is ensured to be separable. This allows one to use the known solutions for the one-dimensional (1D) problem [7–14] in order to construct the solutions in two and higher dimensions (as was done for similar models in the past [15–21]). Two-dimensional eigenfunctions can therefore be expressed as Cartesian products of the 1D eigenfunctions [3], and the corresponding 2D eigenvalues are given by pairwise sums of the 1D eigenvalues.

The 1D spectrum for the Nth order Fibonacci approximant is composed of F_N bands, where $F_N = F_{N-1} + F_{N-2}$ is the Nth Fibonacci number, starting with $F_0 = F_1 = 1$. The edges of each such band correspond to either periodic or antiperiodic boundary conditions. Hence, by direct diagonalization of the two corresponding hamiltonians for a single approximant we obtain the edges of the energy intervals in the spectrum. The 2D and 3D spectra are then calculated as the Minkowski sums of two or three 1D spectra, where the Minkowski sum of two sets A and B is the result of adding every element of A to every element of B, i.e. the set

$$A + B = \{x + y \mid x \in A,\ y \in B\}. \quad (2)$$

Although the spectrum of the 1D Fibonacci model, for any choice of $T \neq 1$, is a totally disconnected set with zero bandwidth and an infinite number of bands, the higher-dimensional spectra exhibit different behaviour for different values of the relative hopping parameter T, including spectra that contain continuous intervals and have a finite measure [2]. A similar situation arises in the case of the well-known *ternary Cantor set* [22], which is constructed iteratively by starting with the closed interval [0,1], and at each iteration removing the open middle thirds of all remaining closed intervals from the previous iteration. The first few approximants that are obtained in this way are $C_0 = [0,1]$, $C_1 = [0,1/3] \cup [2/3,1]$, and $C_2 = [0,1/9] \cup [2/9,1/3] \cup [2/3,7/9] \cup [8/9,1]$, so that after N such iterations one is left with an approximant set C_N consisting of 2^N closed intervals, each of which has a measure $1/3^N$, and therefore the total measure of the set is $(2/3)^N$. The ternary Cantor set itself C_∞, defined as the limit $N \to \infty$ of this

sequence of sets, contains uncountably-many points yet no interval, it is totally disconnected, and its total measure is zero. By simple inspection, one finds that for any finite order Cantor approximant C_N, the Minkowski sum $C_N + C_N$ is the entire interval [0, 2]. One can show that this also holds in the limit $N \to \infty$, namely that $C_\infty + C_\infty = [0, 2]$. Thus, even though C_∞ contains no interval, its sum with itself covers the whole interval from 0 to 2.

For a given dimension n, we identify a sequence of values $1 < T_1^{(nd)} \leq T_2^{(nd)} \leq T_3^{(nd)} \leq T_4^{(nd)}$ corresponding to the following transitions in the spectrum:

- $T_1^{(nd)}$: The value of T below which all bands in the n-dimensional spectrum are of positive, finite measure. For $T > T_1^{(nd)}$ there is at least a finite number of zero measure bands in the spectrum.
- $T_2^{(nd)}$: The value of T above which the number of bands in the n-dimensional spectrum is infinite. An infinite number of bands in a spectrum of finite bandwidth necessarily implies that infinitely many bands are of zero measure, thus $T_2^{(nd)} \geq T_1^{(nd)}$.
- $T_3^{(nd)}$: The value of T above which all bands in the spectrum are of zero measure.[2]
- $T_4^{(nd)}$: The value of T above which the total bandwidth of the spectrum is zero.

We use two different approaches to study the behaviour of the spectrum. In Section 2 we use analytical results derived for the addition of generalized Cantor sets to obtain an upper bound on the transition between a spectrum containing an interval and a nowhere dense spectrum. In Section 3 we use direct numerical calculation of the 2D and 3D spectra of Fibonacci approximants of finite order to extrapolate for the behaviour in the quasiperiodic limit. In an earlier paper [3] we studied only two of the transitions, $T_2^{(nd)}$ and $T_4^{(nd)}$. To find $T_4^{(nd)}$ we used a naive method based on the results of Ashraff et al. [21] for the diagonal tight-binding hamiltonian. The current results include a correction to our previous calculation. In Section 4 we summarize the results, and discuss their expected relation to the nature of eigenfunctions and to quantum dynamics, indicating directions for future work.

2. Analytical bounds for the appearance of continuous intervals in the spectrum

2.1. *Addition of generalized Cantor sets – Known results*

A generalized Cantor set is obtained just like the ternary Cantor set except that the open intervals removed at each iteration are not necessarily the middle thirds of the remaining closed intervals. For each interval removed from the set, one defines a *left* (*right*) *ratio of dissection* as the ratio between the length of the left (right) remaining interval and the length of the original one. Sets for which the left and right ratios are the same are called *central Cantor sets*. In general, the ratios of dissection may vary between the left and right resulting intervals, between different iterations of the process, and between different intervals at the same step. The ternary Cantor set is a central Cantor set with a constant ratio of dissection of 1/3.

We are interested in conditions for the appearance of intervals in the Minkowski sum of n generalized Cantor sets. For central Cantor sets with a constant ratio of dissection a, one can show that the condition for the sum to be an interval is

$$n\frac{a}{1-a} \geq 1 \quad \text{or} \quad a \geq \frac{1}{n+1}. \tag{3}$$

Thus, the ternary Cantor set exactly has the critical value of $a = 1/3$ for which a sum of $n = 2$ central Cantor sets is an interval. Cabrelli et al. [23] found, more generally, a sufficient condition for the existence of an interval in the sum of n generalized Cantor sets, all of which can be constructed with a lower bound a on their ratios of dissection, which is given by

$$(n-1)\frac{a^2}{(1-a)^3} + \frac{a}{1-a} \geq 1. \tag{4}$$

2.2. *Applying Cantor set results to the Fibonacci spectra*

Before using the results quoted above to analyse the Fibonacci spectra, we should note that there exist two important differences between the energy spectra S_N of the Nth order approximants of the 1D Fibonacci quasicrystal, and finite approximants C_N of generalized Cantor sets. The spectrum S_N consists of F_N rather than 2^N energy intervals, and is not contained in the spectrum S_{N-1} of the approximant of order $N-1$. The latter implies that one should take care in defining the proper limit that yields the spectrum S of the Fibonacci quasicrystal itself. Such a definition was given by Sütő [24] (see also Damanik [25]) as

$$S = \bigcap_{N=1}^{\infty} (S_N \cup S_{N+1}). \tag{5}$$

The fact that the number of bands in S_N is F_N rather than 2^N implies that the spectra cannot be constructed by the iterative process described above for generalized Cantor sets, and hence that the ratios of dissection cannot be defined. However, the spectrum S_N of a finite approximant can be padded with additional intervals which can be chosen in a manner that will not disturb the calculation, and will increase the number of intervals to 2^N, as in the Cantor approximant. This allows to calculate backwards and define *effective ratios of dissection*. The additional intervals can be added on either, or both, ends of the spectrum. Thus, the effective ratios of dissection are not uniquely determined.

We have tried using Equation (4) to find a sufficient condition for the higher-dimensional spectra to contain an interval. This would provide a lower bound on $T_3^{(nd)}$ – a value of T below which the condition is satisfied and the n-dimensional spectrum necessarily contains an interval. Unfortunately, as one studies the effective ratios of dissection defined for the 1D spectrum it turns out that regardless of the way in which the approximant spectra are embedded in Cantor approximants, the ratios of dissection are not bounded away from zero, even for small values of T, as shown in Figure 1a. Hence, at this point we do not know how to use the condition of

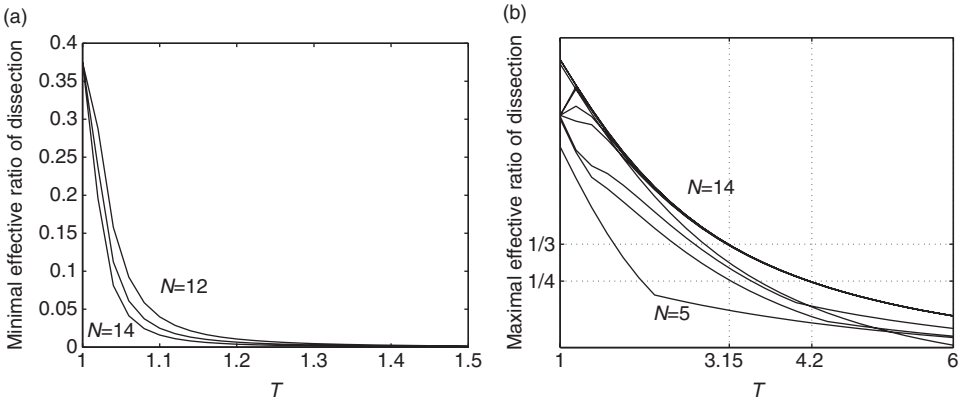

Figure 1. (a) The minimal effective ratio of dissection calculated for the 1D spectra of approximants of order 12–14 for values of T up to 1.5. The sharp drop near $T=1$ means that no value of T satisfies the sufficient condition for obtaining an interval in the higher-dimensional spectra. (b) The maximal effective ratio of dissection calculated for the 1D spectra of approximants of order 5–14 for values of T up to 6. The horizontal dotted lines are drawn at 1/3 and 1/4 to indicate the upper bounds for the value of T at which no intervals are to appear in the 2D and 3D spectra, respectively.

Cabrelli et al. to obtain a lower bound on $T_3^{(nd)}$. Nevertheless, by studying the maximal effective ratio of dissection we can obtain an upper bound for the value of $T_3^{(nd)}$ above which the higher-dimensional spectra do not contain an interval. This is due to the fact that values of T, for which the maximal ratio of dissection fails to satisfy Equation (3), imply that there is no portion of the 1D spectrum which can lead to the existence of an interval in the higher-dimensional spectra. Figure 1b shows the effective maximal ratio for approximants of order $N=5$ ($F_N=8$) to $N=14$ ($F_N=610$). It is evident that the maximal ratio of dissection rapidly converges as a function of the order of the approximant, with almost no difference between the the curves for $N=9$ and above. It is also of interest to note that the maximal ratio is independent of the way in which the approximant spectrum is embedded in a Cantor approximant. The maximal ratio of dissection becomes 1/3 at $T\simeq 3.15$ and 1/4 at $T\simeq 4.2$. Thus, we expect to see the vanishing of intervals in the spectrum at a value of T below these upper bounds for 2D and 3D, respectively.

3. Direct study of the 2D and 3D spectra

We now turn to the direct study of the higher-dimensional spectra. This is done by explicitly calculating the spectra for approximants of finite order. Each pair or triplet of energy bands in the 1D spectrum is summed to yield a single band in the 2D or 3D spectrum, respectively. A set of F_N bands in the 1D spectrum generates $(F_N+1)F_N/2$ bands in the corresponding 2D spectrum, and $(F_N+2)(F_N+1)F_N/6$ bands in the 3D spectrum, with possible overlaps that decrease as T increases. Overlapping bands are merged into single energy intervals to obtain the actual structure of the higher-dimensional spectra. Note that we shall use the term 'bands' to refer to the continuous energy intervals in the spectra,

even though strictly speaking they may be composed of different bands with overlapping energies.

3.1. *Measuring the smallest band in the spectrum to find* $T_1^{(nd)}$

For $T > T_1^{(nd)}$ there is at least one zero-measure band in the spectrum. We therefore measure the smallest band $B_{\min}$ and ask whether it vanishes in the limit of $N \to \infty$. For $T < T_1^{(nd)}$ the length of the smallest band is independent of the order N of the approximant. For $T > T_1^{(nd)}$ it can be described by a power law $B_{\min} \propto F_N^{-\alpha_n(T)}$ with some positive exponent, $\alpha_n(T)$. We locate $T_1^{(nd)}$ by finding the value of T for which α_n vanishes. Figure 2b clearly shows that $1.6 < T_1^{(2d)} < 1.8$, and Figure 2d indicates that $2 < T_1^{(3d)} < 2.6$. Within these bounds, the width of the smallest band oscillates between the two different limiting behaviours.

As T increases and the overlap of bands vanishes, the smallest band in the n-dimensional spectrum is expected to be n times the smallest band of the 1D spectrum. Hence for high values of T the exponents $\alpha_n(T)$ should be independent of the dimension, because the multiplicative factor of n only adds a constant term in the

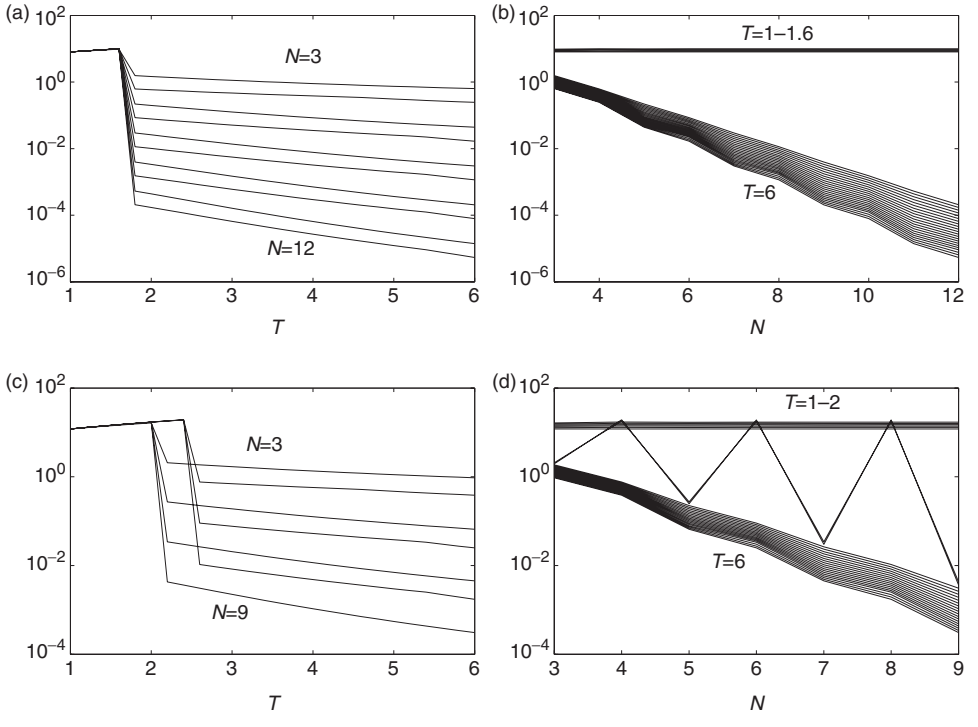

Figure 2. The length of the smallest band $B_{\min}$ in the spectrum of the 2D (top) and the 3D (bottom) Fibonacci quasicrystals. The length of the smallest band is plotted on the left as a function of T for different approximants, and on the right as a function of N for different values of T. The linear slopes in the semi-logarithmic plots as a function of N indicate a power law behaviour, $B_{\min} \propto \tau^{-N\alpha_n(T)}$, where τ is the golden mean. The exponents $\alpha_n(T)$ are plotted in Figure 3.

semi-logarithmic scale. Figure 3 shows the extracted exponents $\alpha_n(T)$, indicating that they indeed coincide for all values of T above $T_1^{(nd)}$. For the periodic case ($T=1$), the spectrum consists of a single band whose width is approximately $2n(1+T)=4n$ independent of the order of approximant and hence $B_{\min}(T=1)\simeq 4n$ independent of the dimension, and $\alpha_n(T=1)=0$.

3.2. *Counting the number of bands to find $T_2^{(nd)}$*

Next we count the number of bands $\#B_n$ in the spectrum and ask whether it tends to infinity or remains finite as N increases. Again, we express this number as a power law of the form $\#B_n \propto F_N^{\beta_n(T)}$, expecting $\beta_n(T)$ to vanish for $T < T_2^{(nd)}$. The existence of such exponents is supported by the linear slopes of the curves in the semilogarithmic plots of Figure 4. For the 1D Fibonacci quasicrystal $\#B_1 = F_N \propto \tau^N$, where τ is the golden mean. In higher dimensions, as the overlap between bands decreases with increasing T, we expect the number of bands to tend to its maximal value, which is approximately $(\#B_1)^2/2$ in 2D, and approximately $(\#B_1)^3/6$ in 3D. Thus the exponents $\beta_n(T)$ should tend to $n\log\tau$ as $T\to\infty$. The dashed horizontal line in Figure 5 indicates the expected limit value for the 2D model which indeed tends to it. For the 3D model the limit is only obtained at significantly higher values of T, indicating that the overlap of bands plays a significant role in the structure of the spectrum even at relatively high values of T. The continuous variation of $\beta_2(T)$ allows us to use smooth extrapolation and find $T_2^{(2d)} \simeq 1.66$, whereas in 3D we can only conclude that $2.0 < T_2^{(3d)} < 2.6$. Combining the fact that $T_2^{(nd)} \geq T_1^{(nd)}$ with the results for the exponents $\beta_n(T)$ as shown in Figure 5, we find that at least in 2D and 3D, $T_2^{(nd)} = T_1^{(nd)}$, and hence that there is no intermediate regime in which the spectrum contains only a finite number of zero-measure bands. For the periodic case $\#B_n = 1$ and hence for $T=1$, $\beta_n = 0$ independent of the dimension.

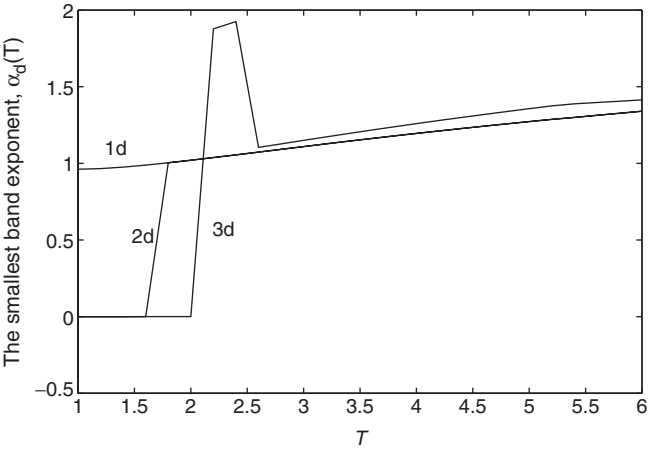

Figure 3. The exponents $\alpha_n(T)$ extracted from Figure 2. The curves for 1D, 2D, and 3D all coincide for values of T above the transition at $T_1^{(nd)}$.

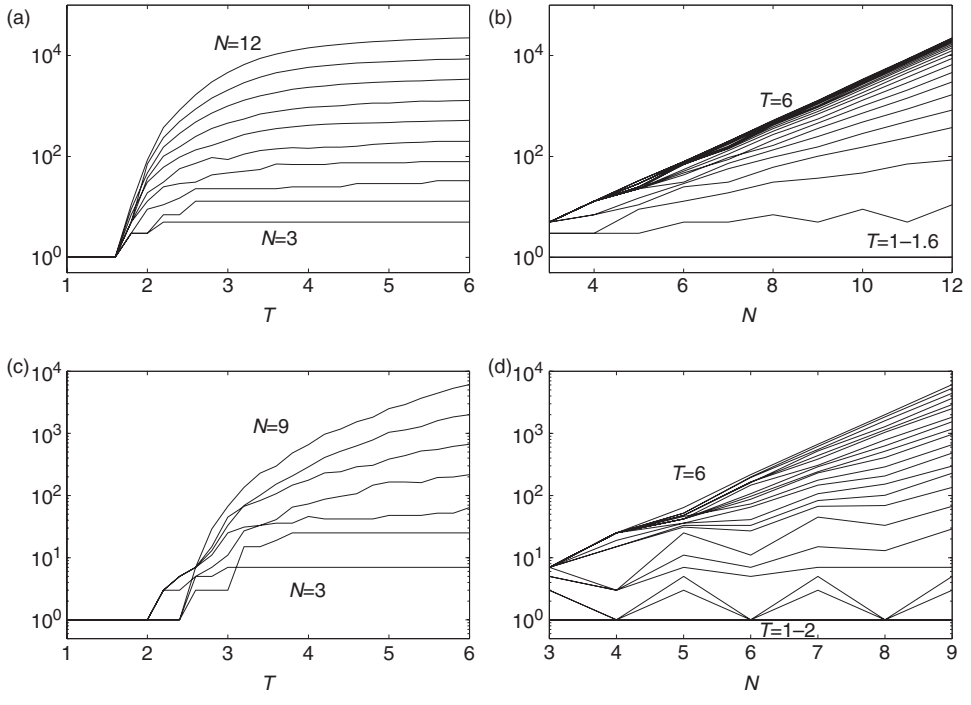

Figure 4. The number of bands $\#B_n$ in the spectrum of the 2D (top) and the 3D (bottom) Fibonacci quasicrystals. The number of bands is plotted on the left as a function of T for different approximants, and on the right as a function of N for different values of T. The linear slopes in the semi-logarithmic plots as a function of N indicate a power law behaviour, $\#B_n \propto \tau^{N\beta_n(T)}$. The exponents $\beta_n(T)$ are plotted in Figure 5.

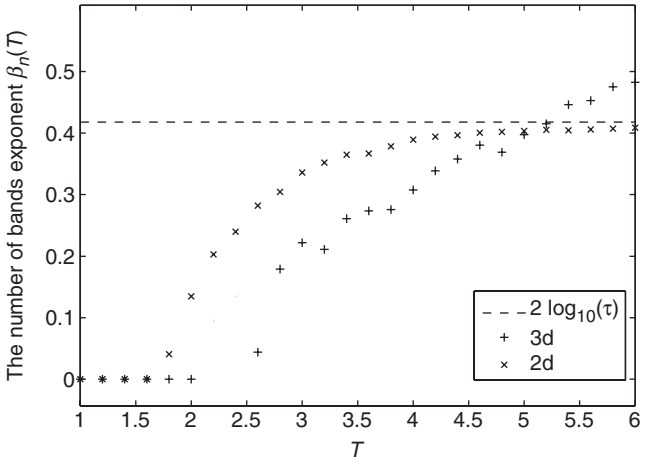

Figure 5. The exponents $\beta_n(T)$, extracted from Figure 4. The horizontal dashed line indicates the expected asymptotic value of $2 \log \tau \simeq 0.418$ for the 2D quasicrystal.

3.3. *Measuring the largest band in the spectrum to find $T_3^{(nd)}$*

For $T > T_3^{(nd)}$ all bands in the spectrum have zero measure. We therefore look at the width of the largest band in the spectrum and ask whether it vanishes as $N \to \infty$. However, since the maximal energy in the spectrum is approximately $n(1+T)$, for small values of T the overlap of bands leads to an increase in the width of largest band as a function of T. To avoid this we normalize the results, dividing by the maximal energy in the spectrum. Thus, for $T > T_3^{(nd)}$, we express the normalized largest band as a power law $B_{\max} \propto F_n^{-\gamma_n(T)}$. Figures 6b and 7 clearly indicate that $T_3^{(2d)} \simeq 2$, but in 3D oscillatory behaviour dominates a large range of values for T, and we cannot determine the transition without extending the analysis to higher order approximants. However, from Figure 6d we can infer that the transition occurs at some value of T below 5, for which we obtained analytically a stricter upper bound of $T_3^{(3d)} \leq 4.2$ as shown in Figure 1b.

As for $B_{\min}$, at large values of T, $B_{\max}$ is also expected to be n times the largest band of the 1D spectrum, and hence the exponents should be independent of dimension. The fact that this does not occur indicates, once again, that the overlap of bands is still significant for values of T as large as 6. At the periodic limit $T=1$ the spectrum consists of a single band and hence $B_{\max}(T=1) \simeq 4n$ independent of the order of approximant and $\gamma_n(T=1) = 0$.

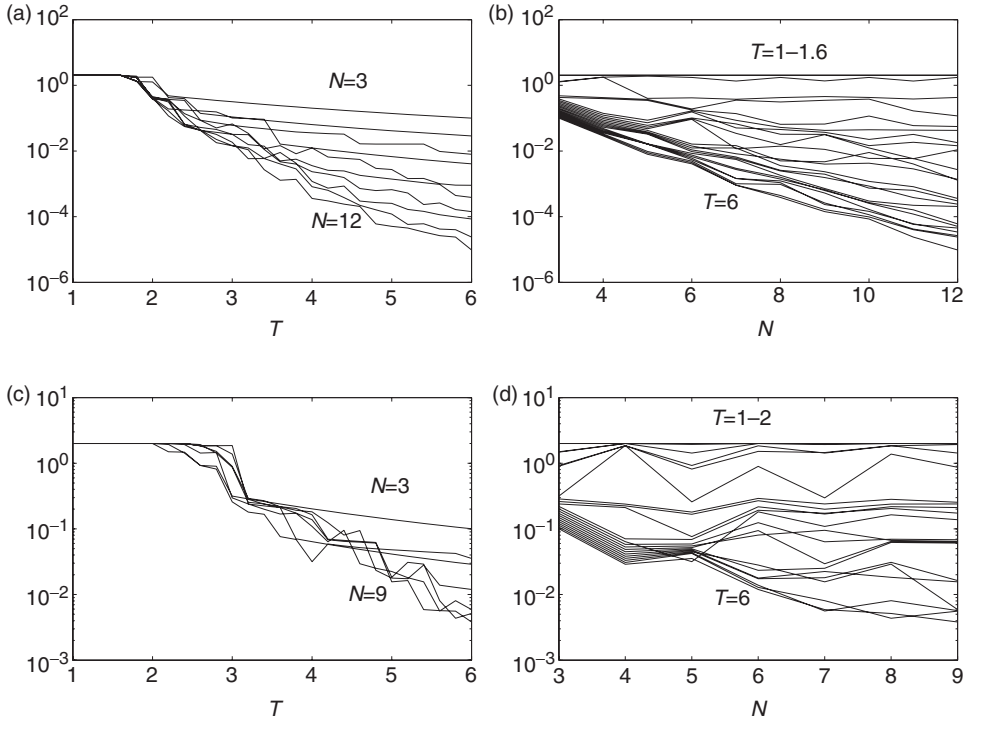

Figure 6. The normalized length $B_{\max}$ of the largest band in the spectrum of the 2D (top) and the 3D (bottom) Fibonacci quasicrystals. $B_{\max}$ is plotted on the left as a function of T for different approximants, and on the right as a function of N for different values of T. The linear slopes in the semi-logarithmic plots as a function of N indicate a power law behaviour, $B_{\max} \propto \tau^{-N\gamma_n(T)}$. The exponent $\gamma_2(T)$ is plotted in Figure 7.

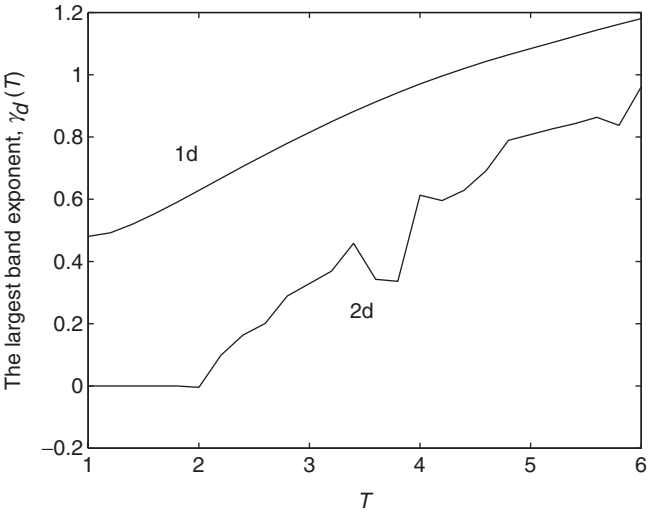

Figure 7. The exponent $\gamma_2(T)$ extracted from Figure 6 and compared with $\gamma_1(T)$. The asymptotic behaviour in which the curves are expected to coincide is not observed for the values of T shown.

3.4. *Calculating the total measure of the spectrum to find* $T_4^{(nd)}$

To find $T_4^{(nd)}$ we measure the total bandwidths of the spectra as N increases, normalizing by $n(1+T)$, and looking for a power law decay of the normalized bandwidth $W \propto F_N^{-\delta_n(T)}$. Figure 8c shows a decrease in the normalized total measure of the spectrum as a function of T in 2D, but Figure 8d shows the total measure in 3D to be almost independent of N for any given value of T. Thus, although the 3D spectrum consists only of zero measure bands for values of T above 5, its total measure remains finite over the entire range of T values studied. The exponents $\delta_n(T)$ are shown in Figure 9. The transition to zero total bandwidth in 2D occurs at $T_4^{(2d)} \simeq 2.6$. In 3D we can only say that $T_4^{(3d)} > 6$. At the periodic limit $T=1$ the spectrum consists of a single band and hence $W(T=1) \simeq 4n$ independent of the order of approximant and $\delta_n(T=1)=0$.

4. Summary and future work

The results of Sections 2 and 3 are summarized as follows

	$T_1^{(nd)}=T_2^{(nd)}$	$T_3^{(nd)}$	Upper bound for $T_3^{(nd)}$	$T_4^{(nd)}$
2D	~ 1.66	~ 2	3.15	~ 2.6
3D	2.0–2.6	≤ 5	4.2	>6

(6)

The transitions between different regimes in the spectrum are expected to reflect on the physical properties of the Fibonacci quasicrystals, on the nature of eigenfunctions and on the dynamics of electronic wave packets. For values of T above the transition $T_3^{(nd)}$

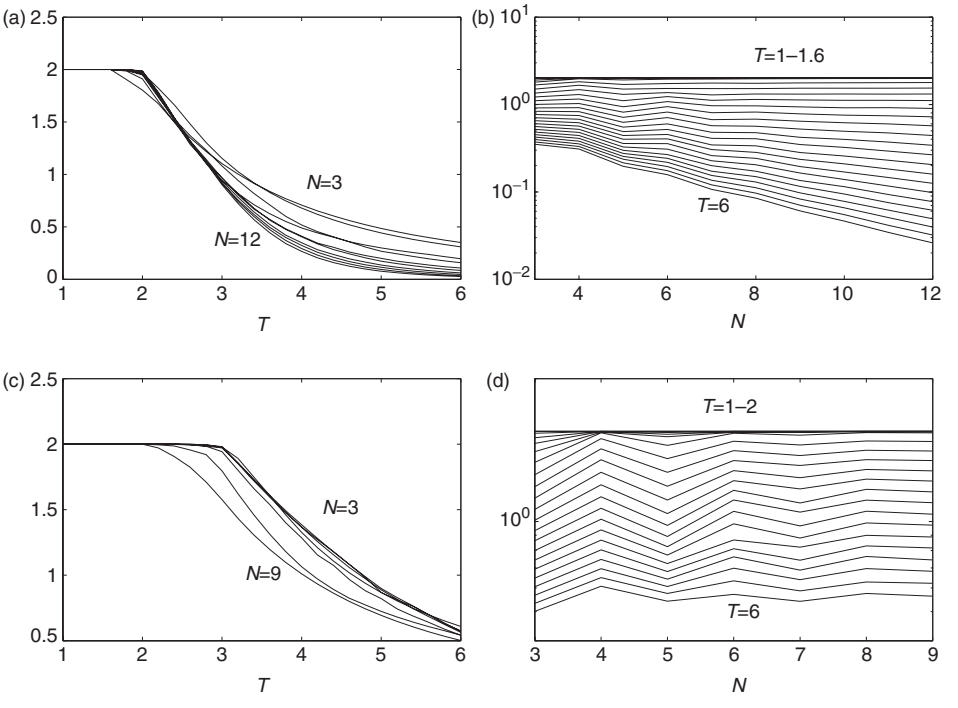

Figure 8. The normalized total bandwidth W of the spectrum of the 2D (top) and the 3D (bottom) Fibonacci quasicrystals. W is plotted on the left as a function of T for different approximants, and on the right as a function of N for different values of T. The linear slopes in the semi-logarithmic plots as a function of N indicate a power law behaviour, $W \propto \tau^{-N\delta_n(T)}$. The exponents $\delta_n(T)$ are plotted in Figure 9.

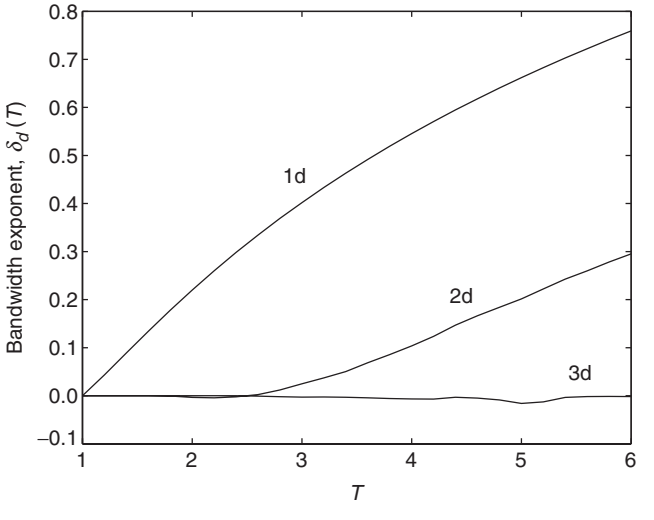

Figure 9. The exponents $\delta_n(T)$, extracted from Figure 8. In 3D it is evident that the transition to zero bandwidth does not occur within the studied range of T values.

the higher-dimensional spectra are similar to the 1D spectrum in being totally disconnected, nowhere dense sets, and hence the eigenfunctions are expected to be critical, and wave packets are expected to display sub-ballistic dynamics, as happens in the 1D case. Note that the last transition $T_4^{(nd)}$ is of no consequence for this matter because the spectrum is nowhere dense both above and below this value. For values of T below the lowest transition point $T_1^{(nd)} = T_2^{(nd)}$, where the spectra are composed of intervals, as in the periodic case, we expect to find extended eigenfunctions, and wave packets are expected to display ballistic dynamics. For the intermediate range between these transitions the spectra contain both intervals and nowhere dense parts, and therefore we expect to find mixed ballistic and sub-ballistic dynamics, and some of the wavefunctions to be extended.

We intend to complement these studies by simulating the dynamics of electronic wavefunctions to find whether transitions between ballistic and sub-ballistic dynamics occur at the points found here. We also intend to use the degeneracy of wavefunctions in the 2D Fibonacci quasicrystal (as hypothesized in [2]) to construct maximally extended wavefunctions; again, we expect to find some qualitative change in the nature of these wavefunctions near the transition points indicated above.

Acknowledgments

We wish to thank David Damanik for showing us the proper way to define the spectrum of the 1D Fibonacci quasicrystal. This research is supported by the Israel Science Foundation through Grant No. 684/06.

Notes

1. The reader is referred to [5,6] for precise definitions of the terms 'crystal' and 'quasicrystal'.
2. Note that the absence of intervals in the spectrum above $T_3^{(nd)}$ does not necessarily correspond to zero total bandwidth. It is in fact possible to use the Cantor set generation process to obtain a totally disconnected set with a finite measure. For example, if at the Nth iteration of the generation process the middle $1/3^N$ part is removed from each of the remaining intervals, one ends with a totally disconnected set whose measure is $\lim \Pi_{k=1}^{\infty}(1 - 1/3^k) \simeq 0.5601$.

References

[1] D. Shechtman, I. Blech, D. Gratias *et al.*, Phys. Rev. Lett. 53 (1984) p.1951.
[2] R. Ilan, E. Liberty, S. Even-Dar Mandel *et al.*, Ferroelectrics 305 (2004) p.15.
[3] S. Even-Dar Mandel and R. Lifshitz, Phil. Mag. 86 (2006) p.759.
[4] R. Lifshitz, J. Alloys Compounds 342 (2002) p.186.
[5] R. Lifshitz, Z. Kristallogr. 222 (2007) p.313.
[6] R. Lifshitz, Found. Phys. 33 (2003) p.1703.
[7] M. Kohmoto, L.P. Kadanoff and C. Tang, Phys. Rev. Lett. 50 (1983) p.1870.
[8] S. Ostlund, R. Pandit, D. Rand *et al.*, Phys. Rev. Lett. 50 (1983) p.1873.
[9] M. Kohmoto and J.R. Banavar, Phys. Rev. B 34 (1986) p.563.
[10] M. Kohmoto, B. Sutherland and C. Tang, Phys. Rev. B 35 (1987) p.1020.
[11] T. Janssen, *The Mathematics of Long-Range Aperiodic Order*, R.V. Moody, ed., Kluwer, Dordrecht, The Netherlands, 1997, p.269.

[12] T. Fujiwara, *Physical Properties of Quasicrystals*, Ch. 6, Z.M. Stadnik, ed., Springer, Berlin, 1999.
[13] J. Hafner and M. Krajcí, *Physical Properties of Quasicrystals*, Ch. 6, Z.M. Stadnik, ed., Springer, Berlin, 1999.
[14] D. Damanik, *Directions in Mathematical Quasicrystals*, M. Baake and R.V. Moody, eds., AMS, Providence, 2000, p.277.
[15] K. Ueda and H. Tsunetsugu, Phys. Rev. Lett. 58 (1987) p.1272.
[16] W.A. Schwalm and M.K. Schwalm, Phys. Rev. B 37 (1988) p.9524.
[17] J.X. Zhong and R. Mosseri, J. Phys: Condens. Matter 7 (1995) p.8383.
[18] S. Roche and D. Mayou, Phys. Rev. Lett. 79 (1997) p.2518.
[19] Yu.Kh. Vekilov, I.A. Gordeev and E.I. Isaev, JETP 89 (1999) p.995.
[20] Yu.Kh. Vekilov, E.I. Isaev and I.A. Gordeev, Mat. Sci. and Eng. 294–296 (2000) p.553.
[21] J.A. Ashraff, J.-M. Luck and R.B. Stinchcombe, Phys. Rev. B 41 (1990) p.4314.
[22] G. Cantor, 'De la puissance des ensembles parfait de points' (On the Power of Perfect sets of Points), Acta Mathematica **4** 381 (1884). English translation reprinted in *Classics on Fractals*, edited by Gerald A. Edgar (Addison-Wesley, 1993).
[23] C.A. Cabrelli, K.E. Hare and U.M. Molter, J. Aust. Math. Soc. 73 (2002) p.405.
[24] A. Sütő, Commun. Math. Phys. 111 (1987) p.409.
[25] D. Damanik, Proc. Sympos. Pure Math. 76, Part 2 (2007) p.505.